Original Article

MOLECULAR METABOLISM

microRNA-205-5p is a modulator of insulin sensitivity that inhibits FOXO function

Fanny Langlet [1,6], Marcel Tarbier [2], Rebecca A. Haeusler [3], Stefania Camastra [4], Eleuterio Ferrannini [4,5], Marc R. Friedländer [2], Domenico Accili [1,*]

ABSTRACT

Objectives: Hepatic insulin resistance is a hallmark of type 2 diabetes and obesity. Insulin receptor signaling through AKT and FOXO has important metabolic effects that have traditionally been ascribed to regulation of gene expression. However, whether all the metabolic effects of FOXO arise from its regulation of protein-encoding mRNAs is unknown.

Methods: To address this question, we obtained expression profiles of FOXO-regulated murine hepatic microRNAs (miRNAs) during fasting and refeeding using mice lacking Foxo1, 3a, and 4 in liver (L-Foxo1,3a, 4).

Results: Out of 439 miRNA analyzed, 175 were differentially expressed in Foxo knockouts. Their functions were associated with insulin, Wnt, Mapk signaling, and aging. Among them, we report a striking increase of miR-205-5p expression in L-Foxo1,3a,4 knockouts, as well as in obese mice. We show that miR-205-5p gain-of-function increases AKT phosphorylation and decreases SHIP2 in primary hepatocytes, resulting in FOXO inhibition. This results in decreased hepatocyte glucose production. Consistent with these observations, miR-205-5p gain-of-function in mice lowered glucose levels and improved pyruvate tolerance.

Conclusions: These findings reveal a homeostatic miRNA loop regulating insulin signaling, with potential implications for *in vivo* glucose metabolism.

Keywords Insulin resistance; Type 2 diabetes; Transcriptional regulation; Liver metabolism; Glucose production; Genetics

1. INTRODUCTION

Insulin resistance predisposes to diabetes and obesity [1]. The pleiotropic effects of insulin are partly mediated by the PI3K/AKT/FOXO1 pathway [1–3]. In liver, insulin decreases glucose production and increases glucose utilization by inhibiting FOXO, whereas insulin resistance activates FOXO, contributing to hyperglycemia and hypertriglyceridemia [4,5]. The protein-coding target genes of FOXO have been studied in detail [6–8]. However, little is known about FOXO regulation of gene expression through micro-RNA (miRNA)-mediated gene silencing.

miRNAs regulate gene expression in physiologic and disease conditions, including insulin-resistant diabetes [9,10]. Interestingly, genome-wide association studies for type 2 diabetes susceptibility loci indicate that most of the diabetes-associated variants localize to non-coding regions [11,12], raising the possibility that miRNAs transcribed from these regions contribute to disease development. Several hepatic miRNAs, including miR-33 [13], miR-122 [14], miR103/107 [15], and miR-802 [16] have been shown to post-transcriptionally control expression of genes involved in metabolism and insulin signaling.

Given the role of FOXO in insulin action, we undertook a systematic search for FOXO-regulated hepatic miRNAs and investigated their metabolic role. Using miRNA profiling of FOXO-deficient mice, we catalogued FOXO-modulated miRNAs and identified miR-205-5p as an endogenous regulator of insulin sensitivity that coordinately targets components of the insulin signaling cascade.

2. MATERIAL AND METHODS

2.1. Experimental model and subject details

2.1.1. Mice

Male mice (9-24-week-old) were maintained on chow (PicoLab rodent diet 20, 5053; Purina Mills). All experiments were approved by Columbia University Institutional Animal Care and Use Committee. *L-Foxo1*, *L-Foxo1,3a,4*, *db/db*, *ob/ob*, and *Sin3a*$^{lox/lox}$:*Sin3b*$^{lox/lox}$ [3,4,6,17] and iL-*Sin3a/3b* mice have been described [6]. C57Bl6, *ob/ob*, *db/db*, and 10-week DIO mice were from The Jackson Laboratories. To overexpress miR-205-5p, we injected 1×10^{11} particles (AAV8.TBG.miRNA (Scramble)-CMV-GFP or AAV8.TBG.miR-205-5p-

[1]Naomi Berrie Diabetes Center and Departments of Medicine, Columbia University, New York, 10032, USA [2]Science for Life Laboratory, Department of Molecular Biosciences, The Wenner-Gren Institute, Stockholm University, 17121, Stockholm, Sweden [3]Naomi Berrie Diabetes Center and Departments of Pathology and Cell Biology, Columbia University, New York, 10032, USA [4]Department of Clinical and Experimental Medicine, University of Pisa School of Medicine, Pisa, Italy [5]CNR Institute of Clinical Physiology, Pisa, Italy

[6] Present address: Center for Integrative Genomics, University of Lausanne, 1015, Lausanne, Switzerland.

*Corresponding author. Naomi Berrie Diabetes Center, 1150 St Nicholas Ave, New York, NY, 10032, USA. E-mail: da230@columbia.edu (D. Accili).

Received July 28, 2018 • Accepted August 7, 2018 • Available online 11 August 2018

https://doi.org/10.1016/j.molmet.2018.08.003

CMV-GFP) in C57Bl6J, and killed the animals after 25 days. For miR-205-5p knock down, C57Bl6J mice were fed high-fat diet for 10 weeks (DIO) (OpenSource Diets, Cat#: D12492), and injected with Custom miRCURY LNA (Exiqon, hsa-miR-205-5p) (Batch nb: 681392) or control (Batch nb: 681393) (15 mg/kg) for 3 days, and killed after 25 days. For miRNA sequencing and miR-205 gain-of-function, *L-Foxo1,3a,4* and C57Bl6J mice were fasted overnight and refed (or not) for 4-hr. For miR-205 loss-of-function, DIO mice were fasted for 5 h. For qPCR, *L-Foxo1*, *L-Foxo1,3a,4* and iL-*Sin3a/3b* mice were fasted overnight; *ob/ob*, *db/db* and DIO mice for 5 h.

2.1.2. Primary hepatocyte culture

Primary hepatocytes were isolated and transfected with plasmids (500 ng/5 $\times$ 10^5 cells, 48-hr) using Lipofectamine2000 as described [18]. *miR-205-5p* was overexpressed with miRCURY LNA miRNA Mimics (15—50nM/5 $\times$ 10^5 cells, 48-hr) against murine *miR-205-5p*; cel-39-3p was used as control. Cells were incubated with 100 uM 8-CPT-cAMP, 1 uM dex, 100 nM insulin or vehicle for 7-hr.

2.1.3. Human studies

Liver biopsies were obtained during bariatric surgery in 10 type 2 diabetics and 10 nondiabetics [19,20]. We extracted RNA with RNA-Later (Ambion Inc., Applied Biosystems, Austin, TX, USA) and obtained plasma samples after an overnight fast. Diabetic patients discontinued treatment 48—72 h before the study. The protocol was approved by the University of Pisa IRB. The nature and purpose of the study were carefully explained to all participants before they provided written consent to participate.

2.2. Method details

2.2.1. Chemicals and antibodies

Reagents were from the following manufacturers: ketamine (KetaSet®), Xylazine (AnaSed®), Medium 199, HBSS, EGTA, HEPES, PenStrep and Gentamycin (Life Technology), Collagen 4 (Worthington), Humulin® R U-100 (Lilly), 8-(4-chlorophenylthio) (CPT)-cAMP, dexamethasone, cycloheximide, bovine serum albumin, D-glucose and sodium pyruvate (Sigma—Aldrich), Lipofectamine2000 (Thermo Fisher), miRCURY LNA (Qiagen) (biotinylated mmu-205-5p and cel-39-3p), anti-FOXO1 (C29H4, # 2880S), anti-Phospho-FoxO1 (Thr24)/FoxO3a (Thr32) (#2599S), anti-Akt, anti-Phospho-Akt (Ser473) (D9E, #4060), anti-SHIP2 (#3397S) and anti-PTEN (#9188S) (Cell Signaling), anti-actin (ab8227) (Abcam).

2.2.2. Plasmids/Viruses

RFP (CTL) and FOXO1 plasmids have been described [21]. Plasmids encoding miTarget™ 3′UTR miRNA Target Clones were from GeneCopoeia (CTRL: CmiT000001-MT05, and FOXO1: Mmi7055419-MT05); AAV8.TBG.eGFP and AAV8.TBG.Cre from Penn Vector Core; AAV8.TBG.miRNA (Scramble)-CMV-GFP and AAV8.TBG.miR-205-5p-CMV-GFP from SignaGene.

2.2.3. RNA and miRNA studies

For qPCR, we used RNeasy kit (Qiagen), GoScript (Promega), and GoTaq® qPCR Master Mix (Promega). Gene expression levels were normalized to TATA-binding protein (TBP) using the $2^{-\Delta\Delta Ct}$ method and are presented as relative transcript levels. For miRNA studies, we isolated RNA with Mirvana (Thermo Fisher, AM1560) or Trizol (Life Technologies). For miRNA sequencing, total RNA was quantified with Ribogreen and libraries were prepared with TruSeq (Illumina, San Diego, CA), quantified with Agilent 2100 Bioanalyzer (Agilent Technologies, Santa Clara, CA) HighSensitivity kit, and sequenced on Illumina HiSeq 2500 Rapid single end 50 cycle flow cell. Low quality tags were altered with FASTX-Toolkit (http://hannon-lab.cshl.edu/fastx_toolkit/). Reads were processed with the pipeline miraligner and mapped to miRBase v.20. For miRNA qPCR, we used miScript II RT Kit (Qiagen) and miScript SYBR Green PCR Kit (Qiagen). Primer assays were from Qiagen. SNORD61 was used to normalize miRNA levels using the $2^{-\Delta\Delta Ct}$ method.

2.2.4. Protein analysis

We extracted proteins in lysis buffer (20 mM Tris-HCl (pH = 7.4), 150 mM NaCl, 10% glycerol, 2% NP-40, 1 mM EDTA, 20 mM NaF, 30 mM Na4P2O7, 0.2% SDS, 0.5% sodium deoxycholate) with Protease/Phosphatase Inhibitor Cocktail (1X, Cell Signaling) and used 0.15 mg in SDS buffer for western blot. We used ImageJ (National Institutes of Health) for densitometry.

2.2.5. Luciferase assays

We transfected hepatocytes with Plasmids encoding miTarget™ 3′UTR miRNA Target Clones (1ug/5 $\times$ 10^5 cells), or miRNA mimics (50 nM), using Lipofectamine 2000 (Invitrogen). 48-hr after transfection, we assayed luciferase with Secrete-Pair™ Dual Luminescence Assay Kit (GeneCopoeia) in an Orion L Microplate Luminometer (Berthold).

2.2.6. Metabolic studies

Glucose production and lipogenesis in primary hepatocyte cultures have been described [18]. We performed glucose and pyruvate tolerance tests in 9—15-week-old male mice after a 16-hr fast using 2 g glucose or pyruvate/kg, and insulin tolerance tests after a 5-hr fast using 0.6 U insulin/kg. Hepatic triglycerides, cholesterol [22], and glycogen were measured as described [5]. We measured glucose with OneTouch (One Touch Ultra, Bayer), triglyceride (Infinity, #TR22421, ThermoFisher), cholesterol (Cholesterol E, #439—17501, Wako Pure chemicals), and NEFA (HR Series NEFA-HR (2), #999—34691, #995—34791, #991—34891, #993—35191, Wako Pure chemicals) by colorimetric assays.

2.2.7. Statistics

Statistical analyses were performed with Prism 5.0 software (Graph Pad). We used two-tailed Student's t-test (two groups), one-way ANOVA followed by Tukey's multiple comparisons (three or more groups), and two-way ANOVA followed by Bonferroni correction (different variables). * = $p < 0.05$, ** = $p < 0.01$, *** = $p < 0.001$. Results are presented as means $\pm$ SEM.

3. RESULTS

3.1. FOXOs regulate hepatic miRNA expression

To identify hepatic miRNAs regulated by FOXOs, we sequenced miRNA from liver of *wild type* (WT) and liver-specific *Foxo1*, *3a*, *and 4* (*L-Foxo1,3a,4*) knockout mice following 12-hr fasting and 4-hr refeeding. FOXOs are active in the fasted state and are inhibited in the refed state through insulin-induced Akt-dependent phosphorylation [23]. Out of 1,289 miRNAs found, we analyzed 439 that were detectable in all samples from fasted and refed mice corresponding to ~34% of total. We detected 109 miRNAs whose expression changed significantly ($p < 0.05$) in fasted *vs.* refed mice, irrespective of genotype (Table S1). Of these, ~57% increased and ~43% decreased. This analysis identified miRNAs known to be regulated by fasting *vs.* refeeding in

liver, such as let-7d, miR-140, miR-210 or miR-22 [24]. When we compared *L-Foxo1,3a,4* and WT mice, irrespective of the feeding state, we found 175 differentially expressed miRNAs ($p < 0.05$) (Table S2). Of these, ~43% increased and ~57% decreased. This analysis detected miRNAs associated with insulin sensitivity [*e.g.*, miR-26a [25], miR-155 [26] and miR-181 [27,28]], gluconeogenesis [*e.g.*, miR-22 [29] and miR-29a [30]], or FOXO1 regulation [*e.g.*, miR-122] [31].

Next, we analyzed differences in fasting *vs.* refeeding expression according to genotype. We detected 52 miRNAs modulated by feeding in WT and 45 in *L-Foxo1,3a,4* (Tables S3 and S4). Of these, 21 were modulated in both genotypes and in the same direction (Figure 1A, Table S5). When we analyzed differences between WT and *L-Foxo1,3a,4* according to the feeding state, we detected 92 miRNAs significantly modulated by genotype during fast and 82 after refeeding (Tables S6 and S7). Of these, 53 were modulated in both conditions and in the same direction (Figure 1B, Table S5). The conclusion from these data is that *L-Foxo1,3a,4* mice fail to regulate expression of a subset of miRNAs in response to fasting and refeeding. Those differences are more pronounced in the fasted state, when FOXOs are active. Finally, we performed a four-way comparison among animals of different genotype (WT *vs. L-Foxo1,3a,4* mice) and metabolic state (fasting *vs.* refeeding) (Tables S5 and S8). We found 50 miRNAs regulated by both genotype and metabolic state: 16 increased in *L-Foxo1,3a,4* mice and during refeeding, suggesting that physiologically they are inhibited by FOXOs; in contrast, 24 decreased in *L-Foxo1,3a,4* mice or during refeeding, indicating that they are induced by FOXOs. 10 miRNA changed in opposite directions in *L-Foxo1,3a,4* mice and during refeeding. Among FOXOs-inhibited miRNA, expression of the miR-96/miR-182/miR-183 cluster increased 3-fold in *L-Foxo1,3a,4* mice. As these miRNAs repress FOXO1 [32], the data provide evidence of feedback regulation of FOXO1 activity. The mir-10 family is inhibited by FOXOs, whereas miR-30, miR-29 and members of the let-7 family are induced by FOXOs (Table S8).

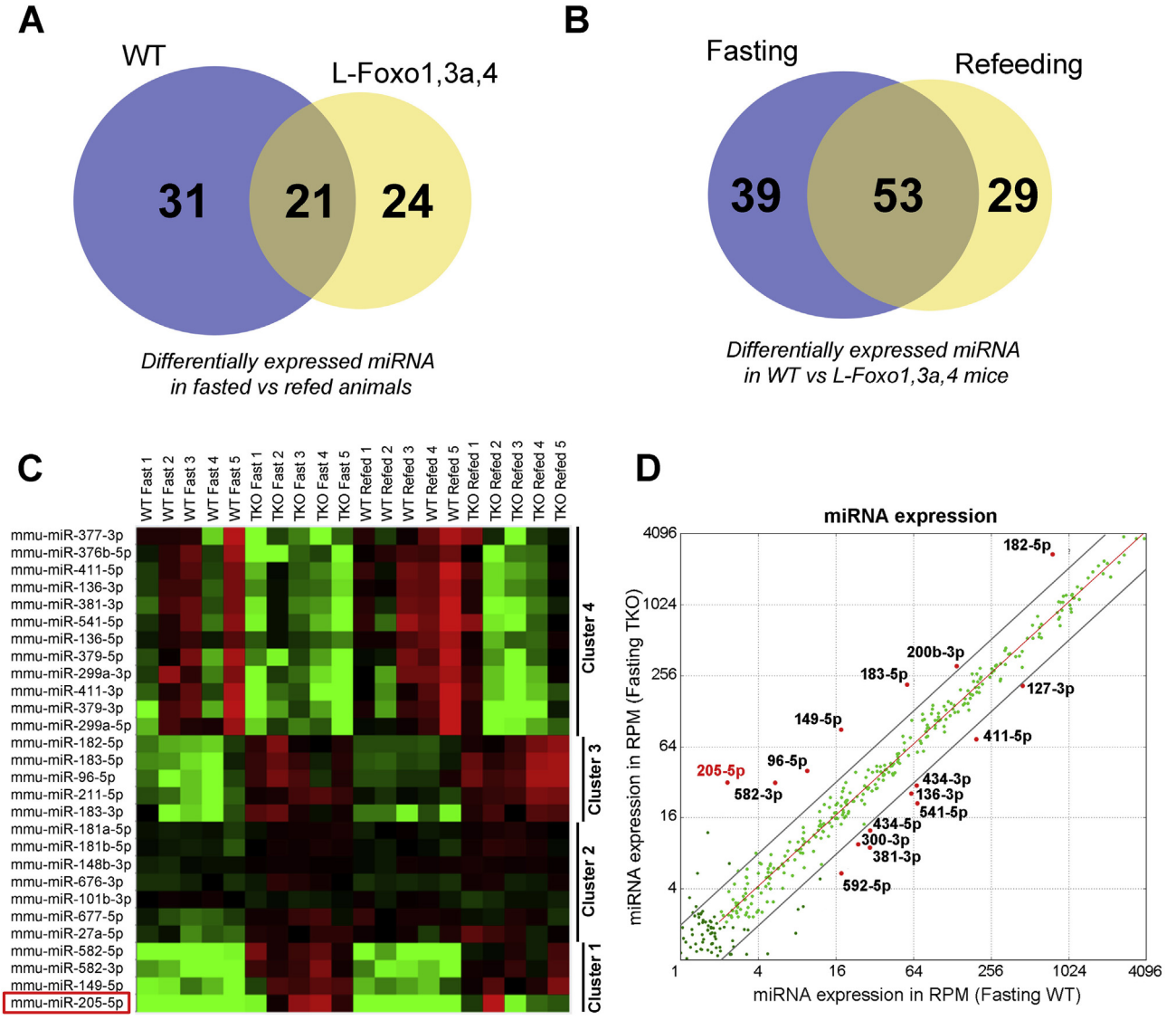

Figure 1: FOXOs modulate hepatic miRNA. A-B, Venn diagrams summarizing differentially expressed miRNAs (**A**) between fasted and refed conditions and (**B**) between WT and *L-Foxo1,3a,4* mice (n = 5 per group). **C**, Heat map of miRNA expression from fasted and refed WT and *L-Foxo1,3a,4* mice. **D**, Scatterplot of miRNA expression in reads per million (RPM) in fasted WT *vs. L- Foxo1,3a,4* mice.

3.2. FOXOs-regulated miRNAs target MAPK, Wnt, and insulin signaling

Next, we built a heat map comparing differentially expressed miRNAs in WT *vs. L-Foxo1,3a,4* mice in fasted and refed conditions using a 5% false discovery rate, and performed hierarchical clustering (Figure 1C). We detected four clusters: clusters 1 and 2 included miRNA whose expression was not regulated by fasting or refeeding but increased in L-Foxo1,3a, 4 mice to a greater (cluster 1) or lesser extent (cluster 2); clusters 3 and 4 included miRNA regulated in the fasted *vs.* fed state whose levels increased (cluster 3) or decreased (cluster 4) in *L-Foxo1,3a,4* mice. The conclusion from these data is that FOXO are able to both induce and inhibit miRNA expression, as they do for gene expression [6]. Moreover, the observation that regulation by FOXO seemingly trumps regulation by the feeding state for clusters 1−2, suggests that the effects of FOXO on miRNA expression can be direct and indirect.

Next, we generated scatterplots of individual miRNAs as a function of their levels in fasted WT *vs. L-Foxo1,3a,4* mice (Figure 1D). From this analysis, we selected miRNAs expressed at levels >5 reads per million that showed a significant ($p < 0.05$) $\log_2$-transformed fold-change ≥ 1 or ≤ -1. Among miRNAs thus selected, 9 were decreased, and 7 increased in *L-Foxo1,3a,4* mice. Gene ontology (GO) analysis and perusal of relevant knockout mouse phenotypes (Tables S9 and S10) identified 3 regulators of Wnt signaling (miR-200b, miR-182 and miR-149) among the FOXO-dependent miRNAs [33,34]. In addition, pathway analysis highlighted insulin signaling, MAPK signaling, and aging/lifespan as targets of these miRNAs, consistent with FOXO-dependent functions [4,35]. The implication of these findings is that physiologically relevant FOXO functions can be mediated through miRNA.

3.3. Pathophysiological regulation of miR-205-5p

Mmu-miR-205-5p topped the list of over-represented miRNAs in fasted *L-Foxo1,3a,4* mice, suggesting that FOXO suppresses its expression (Table S2, Figure S1A). Ontology analysis suggests that miR-205-5p increases P3K/Akt signaling (Table S9). Thus, we selected it for further investigation. Hepatic mmu-miR-205-5p levels are low and don't change with fasting and refeeding in WT mice (Figure S1A). In contrast, in *L-Foxo1,3a,4* mice we observed a 15- to 18-fold increase by RNAseq (Figure S1A) and qRT-PCR (Figure 2A) during fasting, and an ~80% decrease upon refeeding (Figure S1A), indicating that FOXOs suppress hepatic miR-205-5p during fasting. Interestingly, we only saw a 2-fold increase in single knockout *L-Foxo1* mice (Figure 2B), suggesting that the large increase in *L-Foxo1,3a,4* mice is likely due to FOXO3 (FOXO4 levels being very low), or that the three isoforms can compensate for each other. In primary hepatocytes

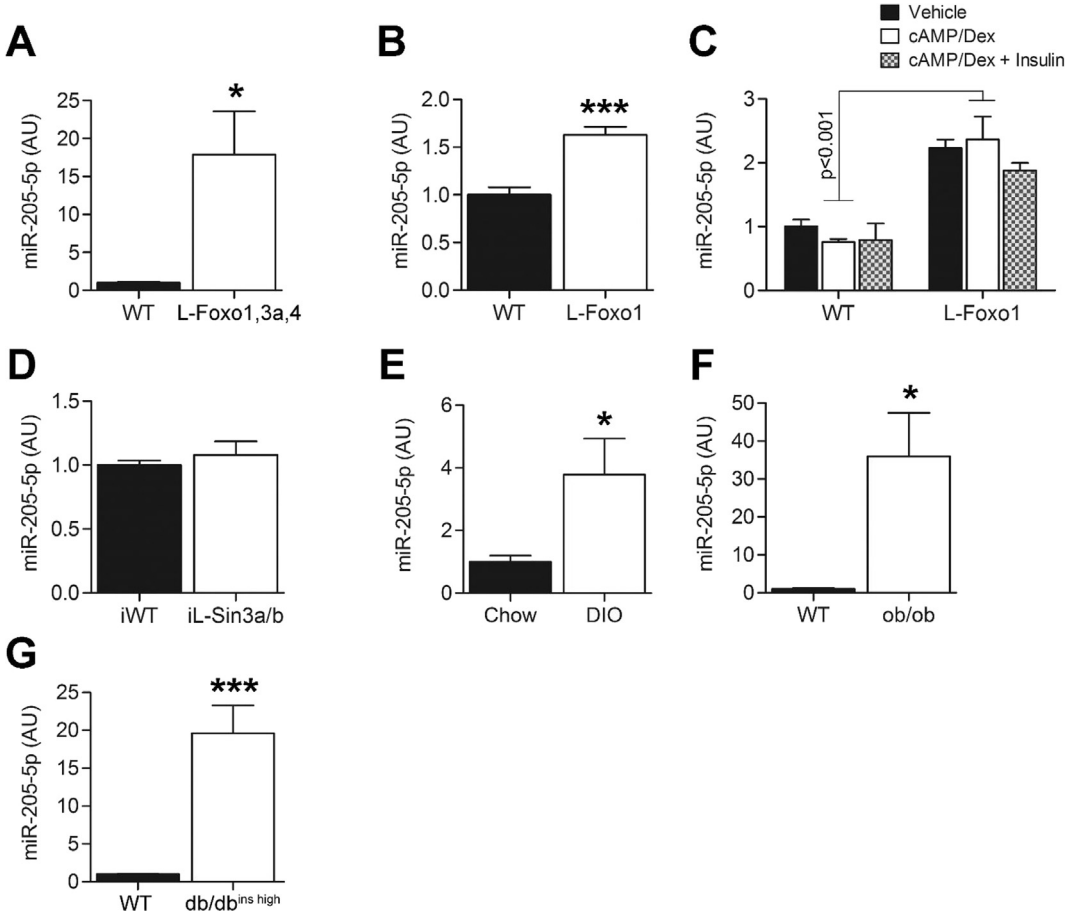

Figure 2: Hepatic miRNA-205 expression in mice and humans. A-B, miR-205-5p expression in liver of WT *vs. L-Foxo1,3a,4* (n = 5 per group) and *L-Foxo1* (n = 7 and 9, respectively) measured by qPCR. **C**, miR-205-5p expression in primary hepatocytes from control WT or *L-Foxo1* mice after 7-hr treatment with vehicle, cAMP/dex, cAMP/dex/insulin (n = 4 per group). **D-G**, miR-205-5p expression in liver of WT *vs.* iL-*Sin3a/b* (**D**) (n = 6 and 7, respectively), chow *vs.* diet-induced obese (DIO) mice (**E**), n = 5 per group), WT *vs. ob/ob* mice (**F**) (n = 5 per group), WT *vs.* hyperinsulinemic *db/db* (ins^{high}) (**G**, n = 7/4, respectively). Data are means ± SEM. *P < 0.05, **P < 0.01, ***P < 0.001.

from *L-Foxo1* mice, mmu-miR-205-5p increased 2-fold (Figure 2C), and the increase was partly reversed by transfecting FOXO1 (Figure S1B). Moreover, mmu-miR-205-5p was not regulated by cAMP/dexamethasone or insulin in primary hepatocytes from L-Foxo1 mice (Figure 2C), failing to mimic the effect of fasting and refeeding. This suggests either that the regulation is lost during hepatocyte culture or that indirect mechanisms mediate miR-205 inhibition by FOXOs *in vivo*.

Mmu-miR-205-5p localizes to chromosome 1 in mice (193, 507, 463—193,507,530 [-]) and humans (209, 605, 478—209,605,587 [+]). Analyses of potential regulatory regions of miR-205-5p in the murine (GRCm38/mm10) and human (GRCh37/hg19) genomes identified several potential FOXO binding sites. However, we failed to detect FOXO binding near miR-205-5p, or in the 5 kb upstream (human chr1:209, 600, 400—209, 609, 275, GRCh37/hg19) by chromatin immunoprecipitation. Interestingly, in these assays we detected the FOXO1 co-repressor, Sin3a [6].

To study the impact of *Sin3a* (and its closely related homolog Sin3b) deletion on mmu-miR-205-5p, we deleted *Sin3a* and *Sin3b* in adult mouse liver by injecting AAV8-TBG-CRE in 8-week-old *Sin3a* $^{lox/lox}$:*Sin3b* $^{lox/lox}$ mice (iL-*Sin3a/b* mice) [6]. We detected no changes in miR-205-5p in overnight-fasted iL-*Sin3a/b* compared to WT mice (Figure 2D). The failure of FOXO to bind candidate regulatory regions of the miR-205 gene, and the lack of miR-205-5p variations in iL-*Sin3a/b* mice, or of regulation by fasting *vs.* refeeding (*in vivo*) or by cAMP/dex *vs.* insulin (*in vitro*) suggest that miR-205-5p is regulated by FOXO indirectly, probably through the inhibition of a potential miR-205 activator.

Given its potential role in insulin signaling, we analyzed regulation of miR-205-5p in obesity, insulin resistance, and type 2 diabetes. In diet-induced obese (DIO), *ob/ob* $^{C57J/B6}$ and hyperinsulinemic *db/db* mice with incipient hyperglycemia (~200 mg/dl) (Figure 2E,F and G, respectively), miR-205-5p increased after a 5-hr fast compared to controls. This is consistent with previous reports showing that hepatic miR-205-5p increases in diabetes-resistant, but not in diabetes-susceptible mice [36].

3.4. Mmu-miR-205-5p inhibits FOXO1 expression and enhances insulin signaling

Given its potential role in PI3k/Akt signaling [37—39], we analyzed the impact of miR-205-5p overexpression on insulin signaling by transfecting primary mouse hepatocytes with miR-205-5p mimics. Overexpression on miR-205-5p in hepatocytes increased basal AKT phosphorylation, without changing protein levels. This effect was blunted by cAMP/dex (Figure 3A—C). The increase in AKT phosphorylation was associated with increased FOXO1 phosphorylation on T24 (Figure 3A,D). miR-205-5p activates PI3K/AKT by targeting PIP3 phosphatases *Pten* [37] and *Ship2* [40]. In primary hepatocytes, miR-205-5p overexpression decreased *Ship2* and increased *Phlpp2* (Figure 3E) but had no effect on *Pten*. Analysis of protein levels by western blot confirmed these data (Figure 3F—H). These results indicate that miR-205-5p enhances insulin signaling *in vitro*.

Moreover, we observed that overexpression of miR-205-5p in primary hepatocytes decreased FOXO1 protein levels in vehicle- and cAMP/Dexamethasone-treated conditions (Figure 3A,I). To validate *Foxo1* inhibition by mmu-miR-205-5p, we analyzed *Foxo1* mRNA in primary hepatocytes transfected with mmu-miR-205-5p and found it to be decreased (Figure 3J, Table S11). miRNAs regulate gene expression through their 5′seed region. Base-pairing of the seed sequence to the target mRNA, usually in the 3′-UTR, leads to its repression. Using TargetScan to predict miRNAs targets [41], we found two potential sites matching the seed region of miR-205-5p in the 3′UTR and in the coding sequence of *Foxo1*. To determine if miR-205-5p targets the *Foxo1* 3′UTR, we used luciferase reporter assays (Figure 3K). Following miR-205-5p transfection, luciferase activity decreased, consistent with the possibility that mmu-miR-205-5p targets the *Foxo1* 3′ UTR (Figure 3K). These results suggest that mmu-miR-205-5p acts in a dual fashion on FOXO1 by increasing Akt-dependent phosphorylation and by inhibiting *Foxo1* expression (Figure 4). These data are consistent with reciprocal inhibition by miR-205-5p and FOXO1.

3.5. miR-205-5p, hepatic glucose production, and *de novo* lipogenesis

As miR-205-5p increases insulin signaling *in vitro*, we analyzed its impact on hepatic glucose production and *de novo* lipogenesis. We found that miR-205-5p overexpression decreased cAMP/dex-induced hepatic glucose production without affecting its inhibition by insulin (Figure 5A), phenocopying *L-Foxo1,3a,4* mice [42]. In contrast to reports in the literature [43], miR-205-5p had no effect on *de novo* lipogenesis (Figure 5B), showing a dissociation between effects on hepatic glucose production and lipogenesis. Moreover, the effect of miR-205-5p to decrease glucose production was dose-dependent, plateauing at 30 nM (Figure 5C).

To understand how miR-205-5p decreases hepatic glucose production, we analyzed gene expression in primary hepatocytes transfected with miR-205-5p mimics at concentrations of 15 or 30 nM (Table S11). Interestingly, induction of gluconeogenic enzymes *G6pc*, *Pck1*, and *Fbp1* by cAMP/dexamethasone was blunted after miR-205-5p transfection (Table S11), consistent with the decrease in hepatic glucose production. Among transcription factors and co-regulators, cAMP/dexamethasone-induced *Foxo1* levels (Table S11), as well as basal *Hnf6*, *Pparγ*, *Foxo4*, *Srebp1c*, and *Crtc2* levels decreased (Table S11), while *Irs2* increased (Table S11). There were no changes in *Gck* and *Pklr*, consistent with the lack of effects on lipogenesis (Table S11). These findings are consistent with the dissociation between effects on glucose *vs.* lipid production, and indicate that miR-205-5p preferentially targets gluconeogenic genes either directly or through increased insulin signaling.

3.6. miR-205-5p decreases fed glucose levels and improves pyruvate tolerance *in vivo*

In view of the effect of miR-205 on hepatic glucose production *in vitro* and its aberrant regulation in obese insulin-resistant mice, we tested the function of miR-205-5p *in vivo* using gain- and loss-of-function experiments. To phenocopy *L-Foxo1,3a,4* mice, we injected AAV8-TBG-miR-205-5p in lean mice, raising miR-205-5p 2-fold in the fasted state, with no differences in the refed state (Figure 6A and S2A—B). This increase did not alter weight (Figure S2C), and body composition (Figures S2D—G). However, it did lower glucose excursion during pyruvate tolerance tests (Figure 6B), suggesting an improvement in gluconeogenesis as observed *in vitro*. It also lowered fed glycemia, starting one week after injection (Figures S2H—I). Three weeks after injection, random fed but not fasted or refed glucose levels were still lower in mice with miR-205-5p gain-of-function (Figure 6C). Fasting cholesterol (Figure 6D) and hepatic cholesterol content (Figure 6E) were also lower, whereas plasma triglyceride (TG) and free fatty acids (Figures S2J—K), as well as hepatic TG content did not change (Figure S2L), consistent with the lack of effects on lipogenesis observed *in vitro*. We also observed increased glycogen content in the refed state compared to WT mice (Figure 6F). To study the mechanism of these effects, we analyzed gene expression (Figure 6G—J, Figure S3). *Gsk3b* decreased and *Irs1* increased during fasting,

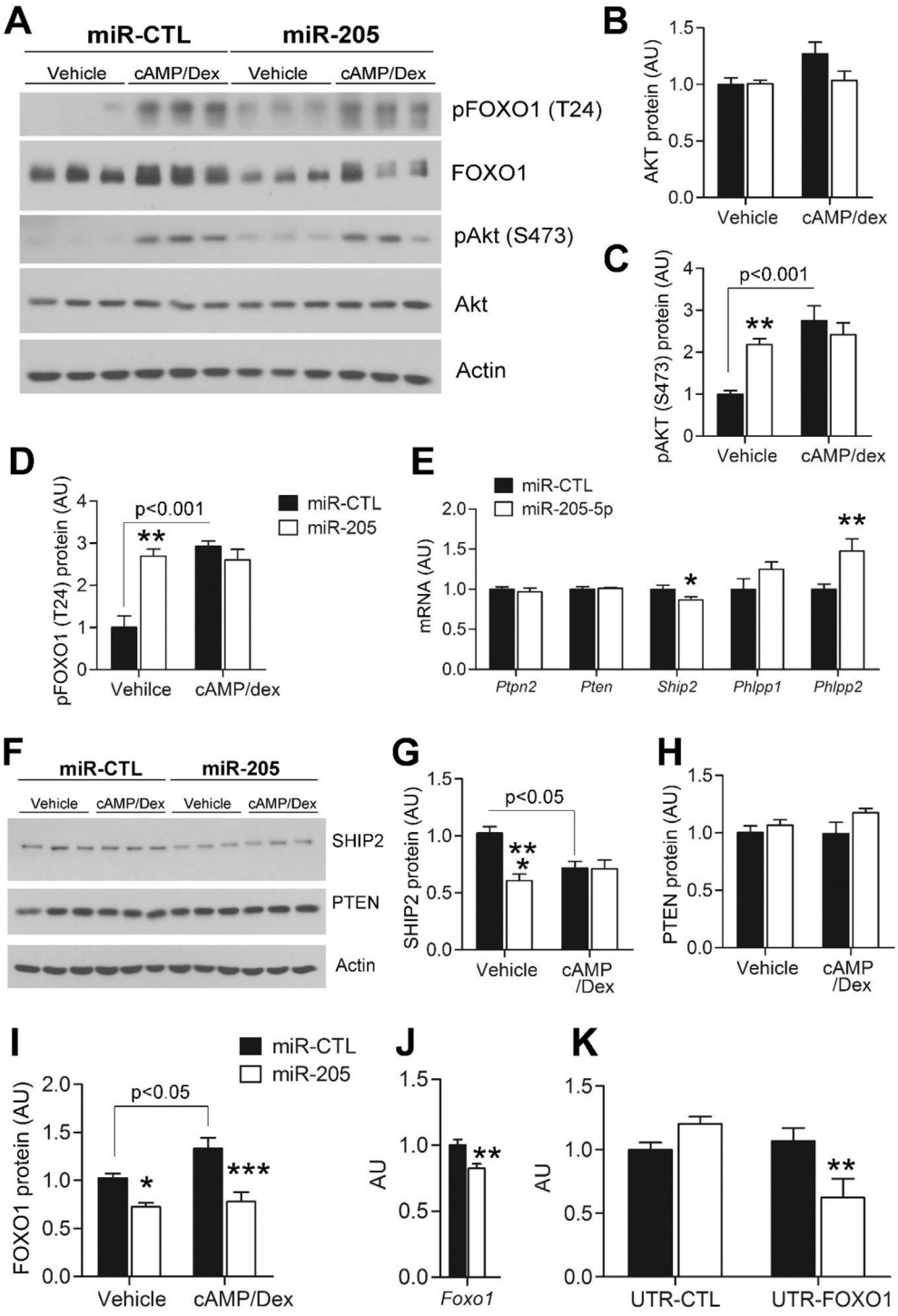

Figure 3: miR-205-5p overexpression in primary hepatocytes activates Akt signaling. A-E, Representative immunoblot (**A**) and quantification (**B-D**) of AKT (**B**), pAKT (**C**), and pFOXO1 (T24) (**D**) levels in primary hepatocytes treated with vehicle or cAMP/dex in the presence or absence of 50 nM miR-205-5p mimics (n = 7, 7, 6, and 3 per group in **B-D,** respectively, from 2 mice). **E,** *Ptpn2*, *Pten*, *Ship2*, *Phlpp1*, *Phlpp2* mRNA in primary hepatocytes in the presence or absence of 50 nM miR-205-5p mimics (n = 8 per group from 2 mice). **F-H**, Representative immunoblot (**F**) and quantification (**G-H**) of SHIP2 (**G**), or PTEN (**H**) levels in primary hepatocytes treated with vehicle or cAMP/dex in the presence or absence of 50 nM miR-205-5p mimics (n = 7 per group). **I**, Quantification of FOXO1 levels in primary hepatocytes treated with vehicle or cAMP/dex in the presence or absence of 50 nM miR-205-5p mimics (n = 7, 7, 6, and 3 per group, from 2 mice). **J,** *Foxo1* mRNA in primary hepatocytes in the presence or absence of 50 nM miR-205-5p mimics (n = 8 per group from 2 mice). **K**, Relative luciferase activity of 3′UTR *Foxo1* in primary hepatocytes transfected with miR-CTL *vs.* miR-205-5p mimics (50 nM). Secreted Gaussia luciferase reporter gene activity was normalized to a secreted Alkaline Phosphatase reporter. Data are means ± SEM. *P < 0.05, **P < 0.01, ***P < 0.001.

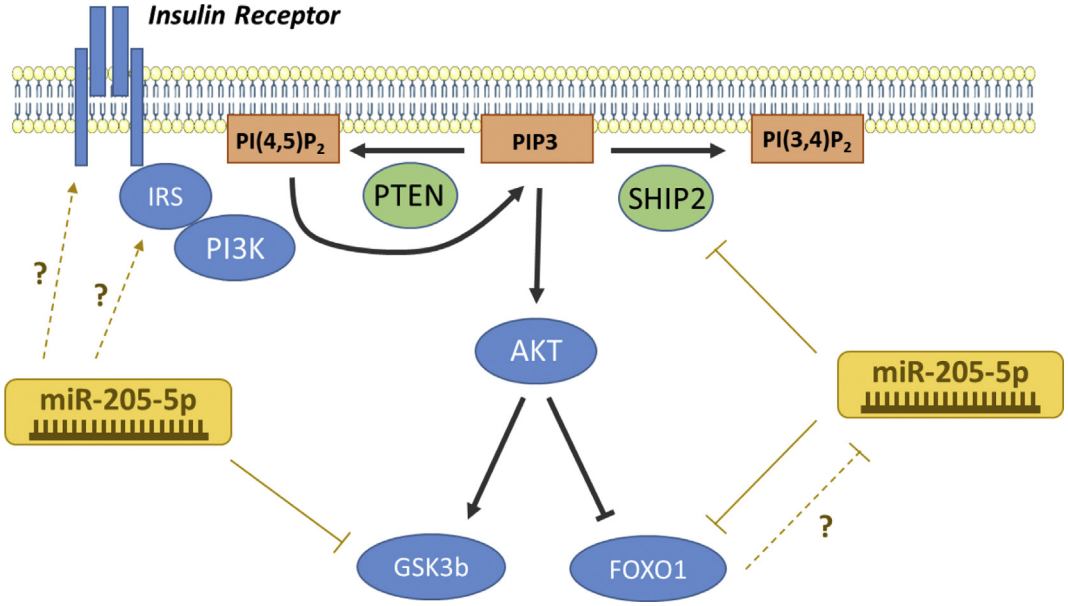

Figure 4: Summary of miR-205-5p regulation of insulin signaling *in vitro*.

whereas *Gck* and *Insr* increased in the refed state (Figure 6G–J, respectively), consistent with increased glycogen content. In contrast with our *in vitro* data, we did not observed changes in gluconeogenic genes (Figure S3), probably due to the modest increase in miR-205-5p achieved *in vivo*, or to indirect mechanisms of mRNA control. Collectively, overexpression of hepatic miR-205-5p in mice is consistent with a decrease in glucose production.

Next, we performed loss-of-function experiments to test whether the increased miR-205-5p expression observed in obese mice affects insulin sensitivity. We injected locked nucleic acids (LNA) antagomirs targeting miR-205-5p in DIO mice, and killed the animals in the fasted state 3 weeks after antagomir administration. Surprisingly, most of the anti-miR-205-5p-treated mice did not gain weight during the first two weeks after injection compared to mice treated with anti-miR-CTL (Figure 7A), even as they maintained similar body composition to control mice (Figures S4A–E). This effect on weight confounds the subsequent analyses and limits our ability to interpret these data. Nonetheless, the animals displayed higher glucose excursions during

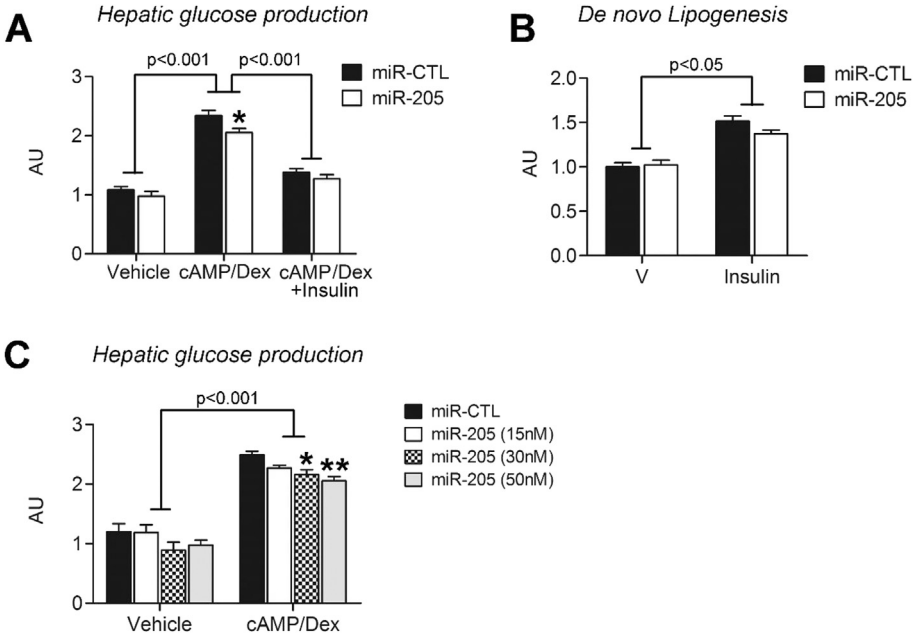

Figure 5: miR-205-5p overexpression in primary hepatocytes decreases hepatic glucose production. A-B, Glucose production (**A**, n = 8 per group from 2 mice) and *de novo* lipogenesis (**B**, n = 6 per group from 2 mice) in primary hepatocytes transfected with miR-CTL *vs.* miR-205-5p mimics (50 nM). **C**, Glucose production (n = 8 per group from 2 mice) in primary hepatocytes transfected with varying concentrations of miR-CTL *vs.* miR-205-5p mimics. Data are means ± SEM. *P < 0.05, **P < 0.01, ***P < 0.001.

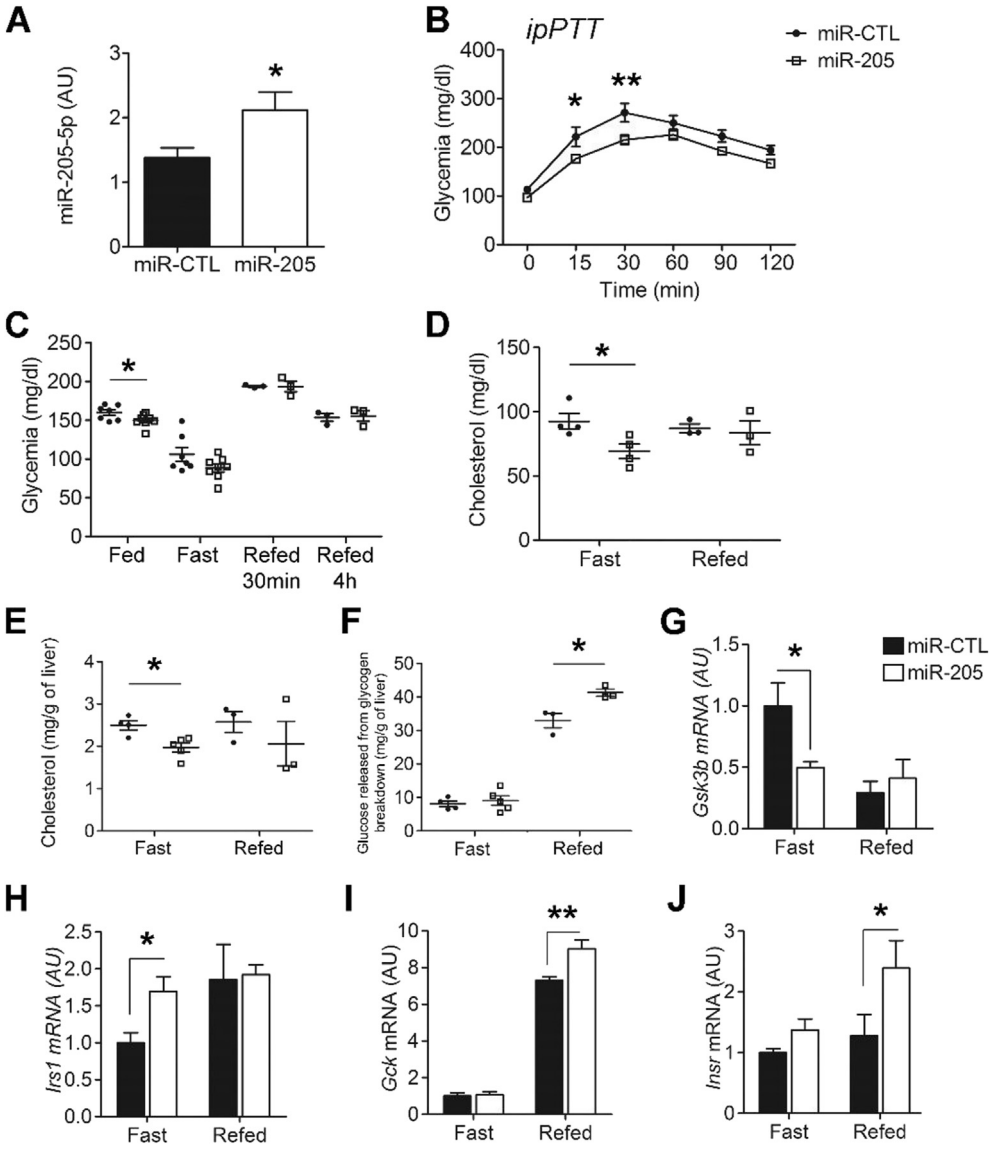

Figure 6: miR-205-5p overexpression in mice improve glucose homeostasis without increasing hepatic fat content. A, Hepatic miR-205-5p expression in C57Bl6 mice after overexpression of miR-CTL *vs.* miR-205 (n = 7 per group). **B**, PTT carried out after an overnight fast in miR-CTL *vs.* miR-205-injected mice (n = 7 per group) 2 and 3 weeks after injection, respectively. **C**, Glucose levels in ad libitum-fed (n = 7 per group), overnight-fasted (n = 7 per group) or 30-min- and 4-hr-refed (n = 3 per group) mice injected with miR-CTL *vs.* miR-205. **D-E**, Plasma and cholesterol levels in 12-hr-fasted (n = 4 per group) and 4-hr-refed (n = 3 per group) mice injected with miR-CTL *vs.* miR-205. **F**, Hepatic glycogen content in 12-hr-fasted (n = 4 per group) and 4-hr-refed (n = 3 per group) miR-CTL *vs.* miR-205 mice. **G-J**, Hepatic *Gsk3* (**H**), *Irs1* (**I**) *Gck* (**J**) and *Insr* (**K**) expression in 12-hr-fasted (n = 4 per group) and 4-hr-refed (n = 3 per group) mice injected with miR-CTL *vs.* miR-205. Experiments in A, and D-J were performed 25 days after injection. Data are means ± SEM. *P < 0.05, **P < 0.01, ***P < 0.001.

glucose and pyruvate tolerance tests (Figure 7B—C). Three weeks after injection, hepatic miR-205-5p decreased 3-fold compared to controls (Figure 7E). 5-hr-fasting plasma triglycerides were lower (Figure 7F), whereas glucose, cholesterol, and free fatty acids did not change (Figure 7G, Figures S4F—G). There were no changes to hepatic cholesterol, triglyceride, and glycogen content (Figures S4H—J). Finally, we analyzed changes in hepatic miR-205-5p targets (Figure S5). *Zeb1* mRNA, a known target of miR-205-5p, as well as *Fbp1* and *Ship2* increased in mice treated with anti-miR-205-5p (Figure 7H—J), consistent with our *in vitro* data and the higher glucose excursions during glucose and pyruvate tolerance tests. Collectively, deletion of hepatic miR-205-5p in DIO mice prevented weight gain but worsened glucose and pyruvate tolerance. The former effect may have blunted the latter.

4. DISCUSSION

FOXOs control gene transcription, but there is limited information on the role of miRNA-mediated gene silencing in their functions. Here we show that FOXOs modulate hepatic miRNA profile, and that miR-205-5p is an important target. We also show that miR-205-5p increases in obese mice. miR-205-5p targets *Foxo1* mRNA for degradation, and defines a potential new mechanism of insulin sensitization.

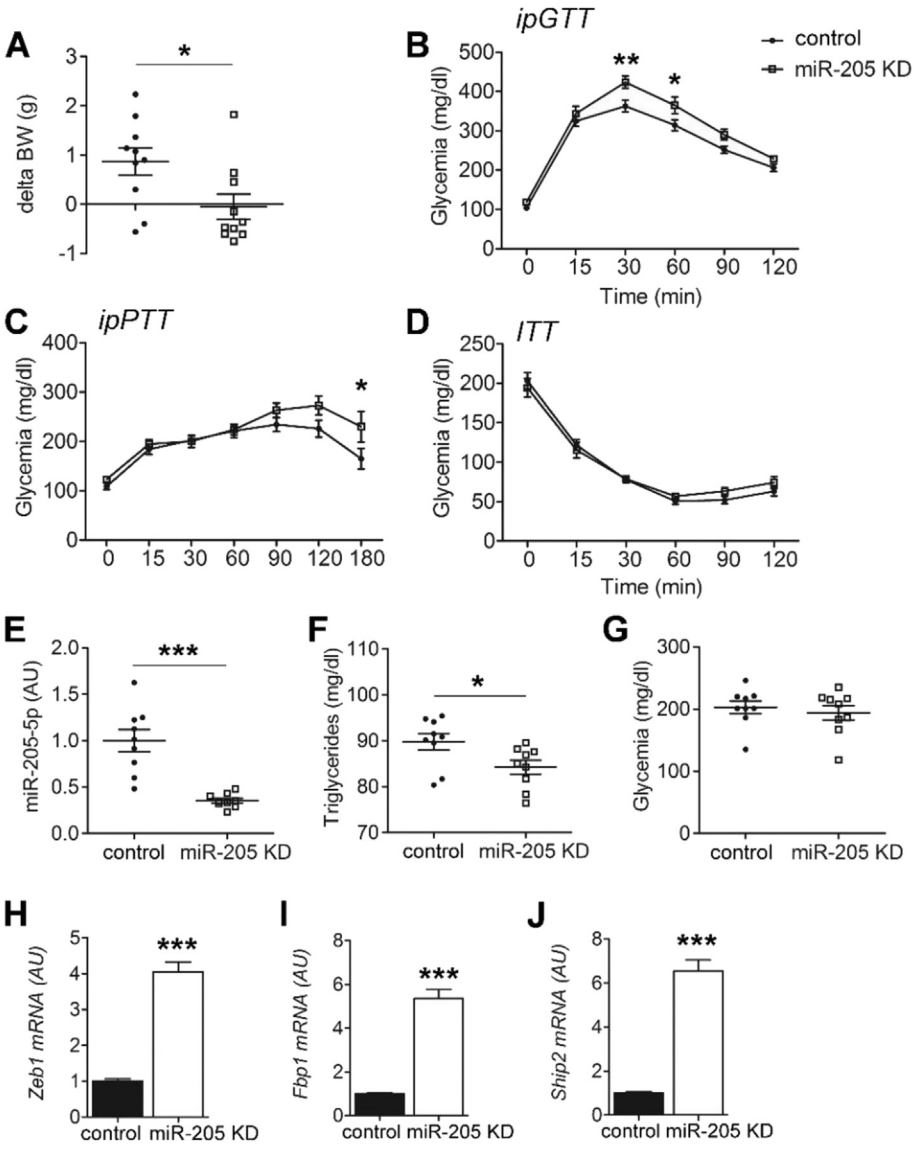

Figure 7: Effects of MiR-205-5p knock-down on glucose homeostasis in DIO mice. A, Differences in body weight among mice injected with control *vs.* miR-205 antagomirs 2 weeks after injection (n = 10 per group). **B-C**, GTT (**B,** n = 9 per group) and PTT (**C,** n = 10 and 8, respectively) carried out after an overnight fast in control *vs.* miR-205 knock down mice (n = 10 per group) 14 and 18 days after injection, respectively. **D,** ITT carried out after a 5-hr-fast in control *vs.* miR-205 knock-down mice (n = 9 per group) 3 weeks after injection. **E**, Hepatic miR-205-5p expression in mice injected with control *vs.* miR-205 antagomirs in 5-hr-fasted (n = 9 per group). **F-G,** Plasma triglyceride (**F**) and glucose (**G**) levels in 5-hr-fasted (n = 9 per group) control *vs.* miR-205 knock-down mice 25 days after injection. **H-K**, Hepatic *Zeb1* (**H**), *Fbp1* (**I**), and *Ship2* (**J**) expression in 5-hr-fasted (n = 8 to 9 per group) control *vs.* miR-205 knock-down mice. Experiments in E-K were carried out 25 days after injection. Data are means ± SEM. *P < 0.05, **P < 0.01, ***P < 0.001.

Our data reveal a heretofore uncharacterized FOXOs-dependent miRNA network. L-*Foxo1*,*3a*,*4* mice display a blunted pattern of miRNA regulation in response to fasting/refeeding. Thus, to the known function of FOXO to regulate expression of protein-coding genes, we add its ability to regulate gene networks through hepatic miRNA. The effects of FOXO are more pronounced in, but not limited to, the fasted state. Whether this is due to indirect effects, or to residual FOXO function in the refed state, remains to be investigated. Interestingly, a subset of FOXO-dependent miRNA appears to play a homeostatic function on metabolism and Akt signaling. We and others have described a homeostatic loop between FOXO and Akt, whereby increased FOXO function begets increased Akt function, and vice versa [23,44,45]. In addition to previously proposed mechanisms [46], the present data indicate that miRNA can mediate this effect. Moreover, FOXO-regulated miRNAs control Wnt and MAPK signaling. As these pathways are known to interact with FOXO [47—50], the present data suggest that miRNA-dependent regulation is a global component of FOXO signaling, and effectively adds up to a second layer of FOXO control over metabolic function.

MiR-205-5p showed profound expression changes in *L-Fox1*,*3a*,*4* mice. miR-205-5p is often co-regulated with the tumor suppressor miR-200 [51], which we also found to be inhibited by FOXO. However, the mechanism by which FOXO inhibit miR-205-5p remains unclear. We have not been able to show direct transcriptional regulation of miR-205 by hepatic FOXO, raising the possibility that the effect is mediated through long—range interactions, or by other transcription factors. It's

likely that FOXOs prevent variations in hepatic miR-205-5p through an indirect mechanism. Moreover, the reciprocal inhibition of FOXO and miR-205-5p establishes a new homeostatic control mechanism. With regard to metabolism, miR-205-5p reportedly regulates lipogenesis by inhibiting glycogen synthase kinase 3β in adipose [52], and acyl-CoA synthetase long-chain 1 (ACSL1) in hepatoma cells [43]. Here, we report that miR-205 gain- or loss-of-function have no clear effect on hepatic lipogenesis, whereas they affect glucose homeostasis, portending a broader role for miR-205 in glycemic control. The early postnatal death of miR-205 knockout animals (Table S10) [53] is consistent with this hypothesis, possibly through impaired glucose production. Regulation of glucose homeostasis by miR-205-5p may depend on its ability to modulate FOXO1 by decreasing its mRNA levels and through Akt activation.

Hepatic miR-205-5p levels also increase in non-diabetic obese mice. These data are consistent with a previous report in mice showing that hepatic miR-205-5p increases in diabetes-resistant, but not diabetes-susceptible mice [36]. Indeed, in a limited cohort of human type 2 diabetics as well as in db/db mice with advanced diabetes, we also observed a decrease of miR205 levels (data not shown). In line with the improvement in glucose homeostasis induced *in vitro* and *in vivo* by miR-205-5p overexpression, there appears to be an inverse correlation between glycemia and hepatic miR-205 levels in the pathogenesis of insulin resistance, similar to miR-320a and miR197 [54,55]. We propose that the role of miR-205-5p in non-diabetic obese individuals is to protect against the development of hyperglycemia. A potential mechanism linking it with FOXO in diabetes is that, when insulin levels rise with insulin resistance, they inactivate FOXO, increasing miR-205. As diabetes advances, hyperglycemia activates FOXO in liver [56], suppressing miR-205. In summary, the present data delineate a mechanism regulating insulin sensitivity through a FOXO-dependent miRNA pathway. The data are consistent with the presence of a regulatory layer through miRNA that recapitulates the principal functions of FOXO through regulation of gene expression.

FUNDING

This work was supported by NIH grants DK57539 and DK63608 (Columbia Diabetes Research Center) and by the Fondation Bettencourt Schueller (F.L.). M.T. and M.R.F. acknowledge funding from the Strategic Research Area program of the Swedish Research Council through Stockholm University. The authors declare no competing financial interests.

ACKNOWLEDGEMENTS

F.L. designed and performed experiments, analyzed data, and wrote the manuscript. R.A.H provided mouse strains, and edited the manuscript. S.C. and E.F. provided human liver tissue specimens, analyzed the data, and wrote the manuscript. M.T. and M.R.F. analyzed data. D.A. designed experiments, oversaw research, and wrote the manuscript.

CONFLICT OF INTEREST

None declared.

APPENDIX A. SUPPLEMENTARY DATA

Supplementary data related to this article can be found at https://doi.org/10.1016/j.molmet.2018.08.003.

REFERENCES

[1] Haeusler, R.A., McGraw, T.E., Accili, D., 2018. Biochemical and cellular properties of insulin receptor signalling. Nature Reviews Molecular Cell Biology 19(1):31. https://doi.org/10.1038/nrm.2017.89.

[2] Dong, X.C., Copps, K.D., Guo, S., Li, Y., Kollipara, R., DePinho, R.A., et al., 2008. Inactivation of hepatic Foxo1 by insulin signaling is required for adaptive nutrient homeostasis and endocrine growth regulation. Cell Metabolism 8(1): 65–76. https://doi.org/10.1016/j.cmet.2008.06.006.

[3] Matsumoto, M., Pocai, A., Rossetti, L., Depinho, R.A., Accili, D., 2007. Impaired regulation of hepatic glucose production in mice lacking the forkhead transcription factor Foxo1 in liver. Cell Metabolism 6(3):208–216. https://doi.org/10.1016/j.cmet.2007.08.006.

[4] Haeusler, R.A., Kaestner, K.H., Accili, D., 2010. FoxOs function synergistically to promote glucose production. The Journal of Biological Chemistry 285(46): 35245–35248. https://doi.org/10.1074/jbc.C110.175851.

[5] Haeusler, R.A., Hartil, K., Vaitheesvaran, B., Arrieta-Cruz, I., Knight, C.M., Cook, J.R., et al., 2014. Integrated control of hepatic lipogenesis versus glucose production requires FoxO transcription factors. Nature Communications 5:5190. https://doi.org/10.1038/ncomms6190.

[6] Langlet, F., Haeusler, R.A., Lindén, D., Ericson, E., Norris, T., Johansson, A., et al., 2017. Selective inhibition of FOXO1 activator/repressor balance modulates hepatic glucose handling. Cell 171(4):824–835.e18. https://doi.org/10.1016/j.cell.2017.09.045.

[7] Nakae, J., Kitamura, T., Silver, D.L., Accili, D., 2001. The forkhead transcription factor Foxo1 (Fkhr) confers insulin sensitivity onto glucose-6-phosphatase expression. The Journal of Clinical Investigation 108(9):1359–1367. https://doi.org/10.1172/JCI12876.

[8] Puigserver, P., Rhee, J., Donovan, J., Walkey, C.J., Yoon, J.C., Oriente, F., et al., 2003. Insulin-regulated hepatic gluconeogenesis through FOXO1-PGC-1alpha interaction. Nature 423(6939):550–555. https://doi.org/10.1038/nature01667.

[9] Fernández-Hernando, C., Ramírez, C.M., Goedeke, L., Suárez, Y., 2013. MicroRNAs in metabolic disease. Arteriosclerosis Thrombosis and Vascular Biology 33(2):178–185. https://doi.org/10.1161/ATVBAHA.112.300144.

[10] Szabo, G., Bala, S., 2013. MicroRNAs in liver disease. Nature Reviews Gastroenterology and Hepatology 10(9):542–552. https://doi.org/10.1038/nrgastro.2013.87.

[11] Cebola, I., Pasquali, L., 2016. Non-coding genome functions in diabetes. Journal of Molecular Endocrinology 56(1):R1–R20. https://doi.org/10.1530/JME-15-0197.

[12] Moszyńska, A., Gebert, M., Collawn, J.F., Bartoszewski, R., 2017. SNPs in microRNA target sites and their potential role in human disease. Open Biology 7(4). https://doi.org/10.1098/rsob.170019.

[13] Dávalos, A., Goedeke, L., Smibert, P., Ramírez, C.M., Warrier, N.P., Andreo, U., et al., 2011. miR-33a/b contribute to the regulation of fatty acid metabolism and insulin signaling. Proceedings of the National Academy of Sciences 108(22):9232–9237. https://doi.org/10.1073/pnas.1102281108.

[14] Esau, C., Davis, S., Murray, S.F., Yu, X.X., Pandey, S.K., Pear, M., et al., 2006. miR-122 regulation of lipid metabolism revealed by in vivo antisense targeting. Cell Metabolism 3(2):87–98. https://doi.org/10.1016/j.cmet.2006.01.005.

[15] Trajkovski, M., Hausser, J., Soutschek, J., Bhat, B., Akin, A., Zavolan, M., et al., 2011. MicroRNAs 103 and 107 regulate insulin sensitivity. Nature 474(7353):649–653. https://doi.org/10.1038/nature10112.

[16] Kornfeld, J.-W., Baitzel, C., Könner, A.C., Nicholls, H.T., Vogt, M.C., Herrmanns, K., et al., 2013. Obesity-induced overexpression of miR-802 impairs glucose metabolism through silencing of Hnf1b. Nature 494(7435): 111–115. https://doi.org/10.1038/nature11793.

[17] Coleman, D.L., 1978. Obese and diabetes: two mutant genes causing diabetes-obesity syndromes in mice. Diabetologia 14(3):141–148.

[18] Cook, J.R., Langlet, F., Kido, Y., Accili, D., 2015. Pathogenesis of selective insulin resistance in isolated hepatocytes. The Journal of Biological Chemistry 290(22):13972–13980. https://doi.org/10.1074/jbc.M115.638197.

[19] Haeusler, R.A., Camastra, S., Astiarraga, B., Nannipieri, M., Anselmino, M., Ferrannini, E., 2015. Decreased expression of hepatic glucokinase in type 2 diabetes. Molecular Metabolism 4(3):222–226. https://doi.org/10.1016/j.molmet.2014.12.007.

[20] Haeusler, R.A., Camastra, S., Nannipieri, M., Astiarraga, B., Castro-Perez, J., Xie, D., et al., 2016. Increased bile acid synthesis and impaired bile acid transport in human obesity. The Journal of Clinical Endocrinology and Metabolism 101(5):1935–1944. https://doi.org/10.1210/jc.2015-2583.

[21] Frescas, D., Valenti, L., Accili, D., 2005. Nuclear trapping of the forkhead transcription factor FoxO1 via Sirt-dependent deacetylation promotes expression of glucogenetic genes. The Journal of Biological Chemistry 280(21):20589–20595. https://doi.org/10.1074/jbc.M412357200.

[22] Folch, J., Lees, M., Stanley, G.H.S., 1957. A simple method for the isolation and purification of total lipides from animal tissues. Journal of Biological Chemistry 226(1):497–509.

[23] Matsumoto, M., Han, S., Kitamura, T., Accili, D., 2006. Dual role of transcription factor FoxO1 in controlling hepatic insulin sensitivity and lipid metabolism. The Journal of Clinical Investigation 116(9):2464–2472. https://doi.org/10.1172/JCI27047.

[24] Craig, P.M., Trudeau, V.L., Moon, T.W., 2014. Profiling hepatic microRNAs in zebrafish: fluoxetine exposure mimics a fasting response that targets AMP-activated protein kinase (AMPK). PLoS One 9(4):e95351. https://doi.org/10.1371/journal.pone.0095351.

[25] Fu, X., Dong, B., Tian, Y., Lefebvre, P., Meng, Z., Wang, X., et al., 2015. MicroRNA-26a regulates insulin sensitivity and metabolism of glucose and lipids. The Journal of Clinical Investigation 125(6):2497–2509. https://doi.org/10.1172/JCI75438.

[26] Lin, X., Qin, Y., Jia, J., Lin, T., Lin, X., Chen, L., et al., 2016. MiR-155 enhances insulin sensitivity by coordinated regulation of multiple genes in mice. PLoS Genetics 12(10):e1006308. https://doi.org/10.1371/journal.pgen.1006308.

[27] Sun, X., Lin, J., Zhang, Y., Kang, S., Belkin, N., Wara, A.K., et al., 2016. MicroRNA-181b improves glucose homeostasis and insulin sensitivity by regulating endothelial function in white adipose tissue. Circulation Research 118(5):810–821. https://doi.org/10.1161/CIRCRESAHA.115.308166.

[28] Zhou, B., Li, C., Qi, W., Zhang, Y., Zhang, F., Wu, J.X., et al., 2012. Down-regulation of miR-181a upregulates sirtuin-1 (SIRT1) and improves hepatic insulin sensitivity. Diabetologia 55(7):2032–2043. https://doi.org/10.1007/s00125-012-2539-8.

[29] Kaur, K., Vig, S., Srivastava, R., Mishra, A., Singh, V.P., Srivastava, A.K., et al., 2015. Elevated hepatic miR-22-3p expression impairs gluconeogenesis by silencing the Wnt-responsive transcription factor Tcf7. Diabetes 64(11):3659–3669. https://doi.org/10.2337/db14-1924.

[30] Liang, J., Liu, C., Qiao, A., Cui, Y., Zhang, H., Cui, A., et al., 2013. MicroRNA-29a-c decrease fasting blood glucose levels by negatively regulating hepatic gluconeogenesis. Journal of Hepatology 58(3):535–542. https://doi.org/10.1016/j.jhep.2012.10.024.

[31] Cao, Q., Zhu, X., Zhai, X., Ji, L., Cheng, F., Zhu, Y., et al., 2018. Leptin suppresses microRNA-122 promoter activity by phosphorylation of foxO1 in hepatic stellate cell contributing to leptin promotion of mouse liver fibrosis. Toxicology and Applied Pharmacology 339:143–150. https://doi.org/10.1016/j.taap.2017.12.007.

[32] Ichiyama, K., Gonzalez-Martin, A., Kim, B.-S., Jin, H.Y., Jin, W., Xu, W., et al., 2016. The MicroRNA-183-96-182 cluster promotes T helper 17 cell pathogenicity by negatively regulating transcription factor Foxo1 expression. Immunity 44(6):1284–1298. https://doi.org/10.1016/j.immuni.2016.05.015.

[33] Cao, D., Jia, Z., You, L., Wu, Y., Hou, Z., Suo, Y., et al., 2016. 18β-glycyrrhetinic acid suppresses gastric cancer by activation of miR-149-3p-Wnt-1 signaling. Oncotarget 7(44):71960–71973. https://doi.org/10.18632/oncotarget.12443.

[34] Peng, Y., Zhang, X., Feng, X., Fan, X., Jin, Z., 2016. The crosstalk between microRNAs and the Wnt/β-catenin signaling pathway in cancer. Oncotarget 8(8):14089–14106. https://doi.org/10.18632/oncotarget.12923.

[35] Martins, R., Lithgow, G.J., Link, W., 2016. Long live FOXO: unraveling the role of FOXO proteins in aging and longevity. Aging Cell 15(2):196–207. https://doi.org/10.1111/acel.12427.

[36] Zhao, E., Keller, M.P., Rabaglia, M.E., Oler, A.T., Stapleton, D.S., Schueler, K.L., et al., 2009. Obesity and genetics regulate microRNAs in islets, liver and adipose of diabetic mice. Mammalian Genome – Official Journal of the International Mammalian Genome Society 20(8):476–485. https://doi.org/10.1007/s00335-009-9217-2.

[37] Cai, J., Fang, L., Huang, Y., Li, R., Yuan, J., Yang, Y., et al., 2013. miR-205 targets PTEN and PHLPP2 to augment AKT signaling and drive malignant phenotypes in non-small cell lung cancer. Cancer Research 73(17):5402–5415. https://doi.org/10.1158/0008-5472.CAN-13-0297.

[38] Jin, C., Liang, R., 2015. miR-205 promotes epithelial-mesenchymal transition by targeting AKT signaling in endometrial cancer cells. The Journal of Obstetrics and Gynaecology Research 41(10):1653–1660. https://doi.org/10.1111/jog.12756.

[39] Zhuo, Z., Yu, H., 2017. miR-205 inhibits cell growth by targeting AKT-mTOR signaling in progesterone-resistant endometrial cancer Ishikawa cells. Oncotarget 8(17):28042–28051. https://doi.org/10.18632/oncotarget.15886.

[40] Yu, J., Peng, H., Ruan, Q., Fatima, A., Getsios, S., Lavker, R.M., 2010. MicroRNA-205 promotes keratinocyte migration via the lipid phosphatase SHIP2. The FASEB Journal 24(10):3950–3959. https://doi.org/10.1096/fj.10-157404.

[41] Agarwal, V., Bell, G.W., Nam, J.-W., Bartel, D.P., 2015. Predicting effective microRNA target sites in mammalian mRNAs. ELife 4:e05005. https://doi.org/10.7554/eLife.05005.

[42] Cook, J.R., Matsumoto, M., Banks, A.S., Kitamura, T., Tsuchiya, K., Accili, D., 2015. A mutant allele encoding DNA binding-deficient FoxO1 differentially regulates hepatic glucose and lipid metabolism. Diabetes 64(6):1951–1965. https://doi.org/10.2337/db14-1506.

[43] Cui, M., Wang, Y., Sun, B., Xiao, Z., Ye, L., Zhang, X., 2014. MiR-205 modulates abnormal lipid metabolism of hepatoma cells via targeting acyl-CoA synthetase long-chain family member 1 (ACSL1) mRNA. Biochemical and Biophysical Research Communications 444(2):270–275. https://doi.org/10.1016/j.bbrc.2014.01.051.

[44] Hay, N., 2011. Interplay between FOXO, TOR, and Akt. Biochimica et Biophysica Acta 1813(11):1965–1970. https://doi.org/10.1016/j.bbamcr.2011.03.013.

[45] Tsuchiya, K., Tanaka, J., Shuiqing, Y., Welch, C.L., DePinho, R.A., Tabas, I., et al., 2012. FoxOs integrate pleiotropic actions of insulin in vascular endothelium to protect mice from atherosclerosis. Cell Metabolism 15(3):372–381. https://doi.org/10.1016/j.cmet.2012.01.018.

[46] Chen, C.-C., Jeon, S.-M., Bhaskar, P.T., Nogueira, V., Sundararajan, D., Tonic, I., et al., 2010. FoxOs inhibit mTORC1 and activate Akt by inducing the expression of Sestrin3 and Rictor. Developmental Cell 18(4):592–604. https://doi.org/10.1016/j.devcel.2010.03.008.

[47] Liu, H., Fergusson, M.M., Wu, J.J., Rovira, I.I., Liu, J., Gavrilova, O., et al., 2011. Wnt signaling regulates hepatic metabolism. Science Signaling 4(158):ra6. https://doi.org/10.1126/scisignal.2001249.

[48] Liu, H., Yin, J., Wang, H., Jiang, G., Deng, M., Zhang, G., et al., 2015. FOXO3a modulates WNT/β-catenin signaling and suppresses epithelial-to-mesenchymal transition in prostate cancer cells. Cellular Signalling 27(3):510–518. https://doi.org/10.1016/j.cellsig.2015.01.001.

[49] Roy, S.K., Srivastava, R.K., Shankar, S., 2010. Inhibition of PI3K/AKT and MAPK/ERK pathways causes activation of FOXO transcription factor, leading to cell cycle arrest and apoptosis in pancreatic cancer. Journal of Molecular Signaling 5:10. https://doi.org/10.1186/1750-2187-5-10.

[50] Zhang, W., Thompson, B.J., Hietakangas, V., Cohen, S.M., 2011. MAPK/ERK signaling regulates insulin sensitivity to control glucose metabolism in Drosophila. PLoS Genetics 7(12):e1002429. https://doi.org/10.1371/journal.pgen.1002429.

[51] Feng, X., Wang, Z., Fillmore, R., Xi, Y., 2014. MiR-200, a new star miRNA in human cancer. Cancer Letters 344(2):166–173. https://doi.org/10.1016/j.canlet.2013.11.004.

[52] Yu, J., Chen, Y., Qin, L., Cheng, L., Ren, G., Cong, P., et al., 2014. Effect of miR-205 on 3T3-L1 preadipocyte differentiation through targeting to glycogen synthase kinase 3 beta. Biotechnology Letters 36(6):1233–1243. https://doi.org/10.1007/s10529-014-1491-8.

[53] Wang, D., Zhang, Z., O'Loughlin, E., Wang, L., Fan, X., Lai, E.C., et al., 2013. MicroRNA-205 controls neonatal expansion of skin stem cells by modulating the PI(3)K pathway. Nature Cell Biology 15(10):1153. https://doi.org/10.1038/ncb2827.

[54] Flowers, E., Gadgil, M., Aouizerat, B.E., Kanaya, A.M., 2015. Circulating micrornas associated with glycemic impairment and progression in Asian Indians. Biomarker Research 3:22. https://doi.org/10.1186/s40364-015-0047-y.

[55] Karolina, D.S., Tavintharan, S., Armugam, A., Sepramaniam, S., Pek, S.L.T., Wong, M.T.K., et al., 2012. Circulating miRNA profiles in patients with metabolic syndrome. The Journal of Clinical Endocrinology and Metabolism 97(12):E2271–E2276. https://doi.org/10.1210/jc.2012-1996.

[56] Haeusler, R.A., Han, S., Accili, D., 2010. Hepatic FoxO1 ablation exacerbates lipid abnormalities during hyperglycemia. The Journal of Biological Chemistry 285(35):26861–26868. https://doi.org/10.1074/jbc.M110.134023.

